Density Functional Studies on Conjugate Addition of $(Me_2CuLi)_2$ to Cyclohexenone: Stereoselectivity and Rate-Determining Step

Seiji Mori[b] and Eiichi Nakamura*[a]

Abstract: The reaction pathway of the conjugate addition of a dimeric cuprate $(Me_2CuLi)_2$ to 2-cyclohexenone has been studied by means of the B3LYP hybrid density functional method, and intermediates and transition structures (TSs) on the potential surface of the reaction have been determined. A lithium/carbonyl coordination complex (**CPli**), a copper/olefin complex retaining a closed cuprate structure (**CPcl**), a copper/olefin complex with an open cuprate structure (**CPop**), and the TS of C–C bond formation (**TScc**) have been located along the gas-phase pathway leading to the conjugate addition product (**PD**). We studied two diastereoisomeric pathways, and found that the pathway that results in the axial placement of the nucleophilic methyl group in the product was favored throughout the course of the reaction, except in the product complex. Thus, the stereoselectivity of the conjugate addition to cyclohexenone originates from the stereochemical preference of the final, rate-limiting C–C bond formation stage that mainly reflects the steric factors in the formation of 3-methylcyclohexanone enolate in its half-chair form (**TSccax**). Comparison of the calculated and experimental values for ^{13}C NMR chemical shift and kinetic isotope effects strongly suggests that the copper/olefin complex of the **CPop** structural type is the reactive intermediate that directly forms the product. Thus, the open complex **CPop**, rather than the closed complex **CPcl** hitherto considered, is a direct precursor of the product and crucial for the stereoselectivity of the conjugate addition. On the basis of theory and experiments, transition-state models for the conjugate addition to substituted cyclohexenones are provided.

Keywords: conjugate additions · cuprates · density functional calculations · enones

Introduction

Conjugate addition of organocuprate occupies a uniquely important position in organic synthesis because of its ability to stereoselectively deliver a carbanionic center to create a new chiral center. Numerous syntheses of complex natural products[1] crucially rely on diastereoselectivity of the conjugate additions, as illustrated by the stereoselective synthetic step in our cortisone synthesis (Scheme 1).[2] Scheme 2 illustrates the simplest, textbook examples of high diastereoselectivities.[3, 4] In spite of the critical importance of stereoselectivity in synthetic applications, understanding of the origin of the selectivity has been very poor, and no consensus has been achieved.[5]

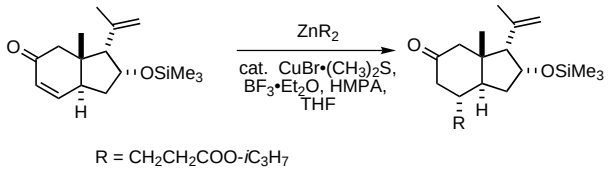

R = CH_2CH_2COO-*i*C_3H_7

Scheme 1.

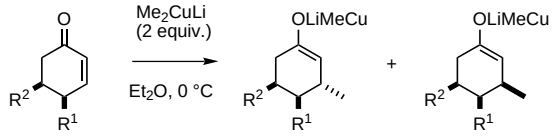

	trans		*cis*
(a) R^1 = Me, R^2 = H	91	:	9
(b) R^1 =H, R^2 = Me	98	:	2

Scheme 2.

Upon a low-level analysis, the diastereoselectivity in Schemes 1 and 2a appears to reflect the product stability. However, the selectivity in Scheme 2b apparently defies this

[a] Prof. E. Nakamura
Department of Chemistry, The University of Tokyo
Hongo, Bunkyo-ku, Tokyo 113-0033 (Japan)
Fax: (+81) 3-5800-6889
E-mail: nakamura@chem.s.u-tokyo.ac.jp
WWW: http://www.chem.s.u-tokyo.ac.jp/~common/Theo/Cj2/title
for 3D pictures and coordinates to be retrieved.

[b] Dr. S. Mori
Department of Chemistry, Emory University
Atlanta, GA 30322 (USA)

Supporting information for this article is available on the WWW under http://www.wiley-vch.de/home/chemistry/ or from the authors.

0947-6539/99/0505-1534 $ 17.50+.50/0 *Chem. Eur. J.* **1999**, *5*, No. 5

hypothesis. On a more advanced level of analysis, the selectivity in Scheme 2b has been rationalized in two ways. One interpretation assumes a transition state **A** which gives the *trans* diastereomer (Scheme 3).[6] While this interpretation

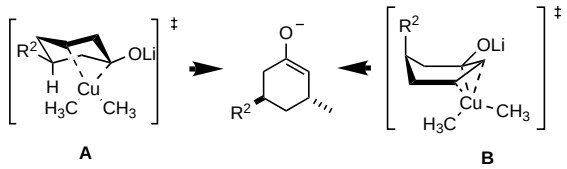

Scheme 3.

is accepted in one community, a different opinion may be held in another, where a boatlike structure (cf. **B**) is assumed.[7, 8]

While the analysis of the stereoselectivity has remained speculative, the kinetics and thermodynamics of the reaction have been studied in considerable depth. The kinetic studies by Krauss and Smith revealed a mechanism [Scheme 4, Eqs (1) and (2)),[9] where an intermediate **D** (or kinetically

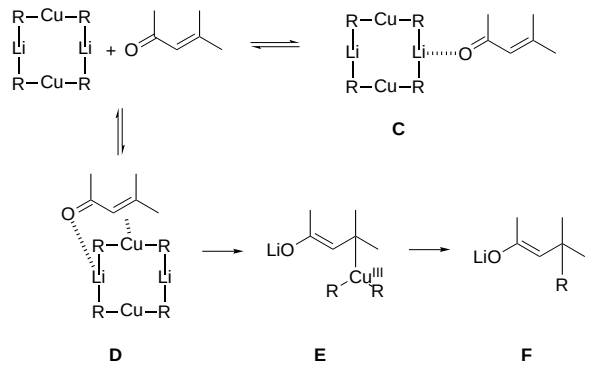

Scheme 4.

$$(R_2CuLi)_2 + \text{enone} \underset{k_{-1}}{\overset{k_1}{\rightleftharpoons}} \text{"intermediate"} \xrightarrow{k_2} \text{product} \qquad (1)$$

$$K = k_1/k_{-1}$$

$$-\frac{d[\text{intermediate}]}{dt} = \frac{kK[(CH_3)_2Cu_2Li_2]}{1+K[(CH_3)_2Cu_2Li_2]}[\text{enone}] \qquad (2)$$

indistinguishable multiple intermediates) formed in equilibrium with the starting material goes through an irreversible step (including C–C bond formation) to give the conjugate adduct **F**.[10] A lithium/carbonyl complex **C** forming in equilibrium with starting materials does not directly give the product, and instead a copper/olefin complex (conventionally formulated as) **D** goes to the product though a Cu^{III} intermediate or a transition state represented by a general structure **E**. This picture was supported by subsequent NMR studies (cf. Scheme 10)[11–13] including the notable recent studies by Krause who identified intermediates related to **D**.[14] Enone/cuprate complexes of closed nature, such as **D**, have often been assumed to exist, based on intuition and computational results.[11d, 15] The relative magnitude of the rate constants was also assessed ($k_1/k_{-1} = 1.5,\ k_{-1} > k_2$).[13] Using their elegant method, Singleton et al. recently determined the kinetic isotope effects in the conjugate addition to cyclohexenone and concluded that the rate-limiting step is C–C bond formation by reductive elimination of a copper(III) intermediate such as **E**.[16] This step must correspond to the Krauss/Smith second energy barrier (k_2).

Unfortunately, it has so far not been possible to consolidate the mechanistic studies on simple substrates and the stereochemical questions in larger systems. To do so, quantum-mechanical calculations of a system close enough to reality are needed, which combine structural, energetic, and theoretical information. Our recent theoretical studies on the simplest substrate (acrolein) provided the first step toward this goal.[17] We now address a system involving a lithium cuprate cluster and 2-cyclohexenone, which provides the first opportunity to study the stereochemistry and the physicochemical characteristics of the conjugate addition in reference to the known experimental data.[18]

In the present studies, we will discuss the origin of the diastereoselectivity of the conjugate addition of a Me_2CuLi dimer to cyclohexenone in terms of energetics and structures obtained for the most realistic models studied by high-level quantum-mechanical calculations (density functional theory, DFT). The present studies revealed the identity of the intermediate in solution which goes directly into the product (as **CPop**), and provided a concrete molecular picture of the rate- and stereochemistry-determining step of the conjugate addition (as **TScc**). The transition-state models for the diastereoselective conjugate addition will be provided based on theoretical and experimental results.

Chemical Models and Computational Details

We have chosen 2-cyclohexenone as our model substrate. The conjugate additions to 2-cyclohexenone derivatives have been the most widely studied experimentally because of the defined conformation of six-membered rings, as well as the abundance of six-membered rings in natural products. It is rather unfortunate that the physical organic studies on the conjugate addition have been undertaken for unreactive,[9, 11–13] highly substituted 2-cyclohexenone derivatives. The parent compound is too reactive to be studied in detail for the mechanism.

As a cuprate model, we mainly studied Me_2CuLi dimer, and also briefly examined a small cluster EtMeCuLi for comparison (which did not affect the conclusion, hence the data will not be shown). Our previous theoretical studies[17] indicated that other cluster models (Me_2CuLi and $Me_2CuLi \cdot LiCl$) will also show reactivities similar to $[Me_2CuLi]_2$.

There are two olefinic faces available for substituted 2-cyclohexenone to receive the attack of a cuprate reagent (see Scheme 5): an attack eventually placing the nucleophilic methyl group at the axial site of the C^3 carbon atom in the final products in its stable chair conformation (conventionally called axial attack), and one placing it at the equatorial site (equatorial attack).

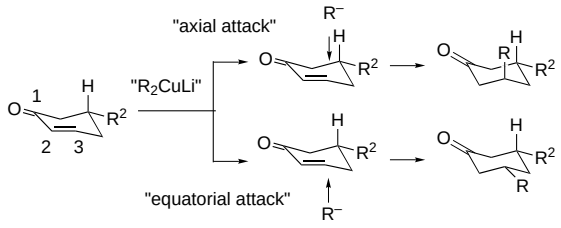

Scheme 5.

We considered the two pathways for the parent cyclohexenone. (Note that the experimental conformational marker group (R^2) is not necessary in the theoretical studies.)

Computational and theoretical analyses followed the protocol previously discussed in great detail.[19] The calculations were performed by the Gaussian 94 program[20] with DFT using the restricted B3LYP method.[21, 22] The 321A basis set[19, 23, 24] was used for structure optimization, normal coordinate analysis for all stationary points, and the 631A basis set[19, 23, 24] was used for single-point energy evaluation and natural population analysis.[25] For two important transition structures (TSs), **TSccax** and **TScceq**, the structure optimization and normal coordinate analysis were also carried out with the 631A basis set to obtain essentially the same results.[26] Note that the energetic error associated with comparison of conformational isomers, which we will give for axial and equatorial pathways, is small enough to make the results reliable for comparison with experimental selectivity.[27] **TSccax** and **TScceq** were also examined with the MP4SDQ single-point calculations with the Ahlrichs SVP all-electron basis set[24]for the copper element and 6-31G basis sets[23] for the other elements.

Kinetic isotope effects[28] were computed by the Bigeleisen–Mayer equation[29] with Wigner tunnel correction [Eq. (3)], based on the calculated frequencies scaled by 0.945 at the B3LYP/321A level and by 0.9614 at the B3LYP/631A level,[30] respectively. In this equation, $u_i = hv_i/kT$, v_i is frequencies in cm^{-1}, $v_i^{\neq}$ is the imaginary frequency for the transition states in cm^{-1}, T is absolute temperature in K, h is Planck's constant, and k stands for the Boatsman constant. The original Bigeleisen–Mayer equation without tunnel effect consideration [Eq. (4)] was also used to evaluate the tunneling effect. The largest and the second largest deviations

$$k_L / k_H = \frac{\nu_{1L}^{\ddagger}}{\nu_{2L}^{\ddagger}} \prod_i^{3n-7} \left[\frac{u_{1i}^{\ddagger}}{u_{2i}^{\ddagger}} \frac{e^{-u_{1i}^{\ddagger}/2}}{e^{-u_{2i}^{\ddagger}/2}} \frac{1-e^{-u_{2i}^{\ddagger}}}{1-e^{-u_{1i}^{\ddagger}}} \right] \prod_i^{3n-6} \left[\frac{u_{2i}}{u_{1i}} \frac{e^{-u_{2i}/2}}{e^{-u_{1i}/2}} \frac{1-e^{-u_{1i}}}{1-e^{-u_{2i}}} \right] \left(1 + \frac{1}{24} \left(\frac{h\nu_{1L}^{\ddagger}}{kT} \right)^2 \right) \Big/ \left(1 + \frac{1}{24} \left(\frac{h\nu_{2L}^{\ddagger}}{kT} \right)^2 \right) \quad (3)$$

$$k_L / k_H \approx \frac{\nu_{1L}^{\ddagger}}{\nu_{2L}^{\ddagger}} \prod_i^{3n-7} \left[\frac{u_{1i}^{\ddagger}}{u_{2i}^{\ddagger}} \frac{e^{-u_{1i}^{\ddagger}/2}}{e^{-u_{2i}^{\ddagger}/2}} \frac{1-e^{-u_{2i}^{\ddagger}}}{1-e^{-u_{1i}^{\ddagger}}} \right] \prod_i^{3n-6} \left[\frac{u_{2i}}{u_{1i}} \frac{e^{-u_{2i}/2}}{e^{-u_{1i}/2}} \frac{1-e^{-u_{1i}}}{1-e^{-u_{2i}}} \right] \quad (4)$$

of -0.007 (C^a) and -0.002 (C^3), respectively (for carbon numbering, see Table 1) were noted for **TSccax** in reference to **CPopax**. The scale factor of 0.945 was derived from the product of the scale of 0.9614 for B3LYP/6-31G(d) frequencies[30] and the ratio of B3LYP/631A frequencies with B3LYP/321A frequencies for the TS in the addition of $(Me_2CuLi)_2$ to acrolein.[17]

For NMR chemical shift calculations, we used gauge-including atomic orbital (GIAO)-B3LYP method[31] combined with the Ahlrichs DZP basis set[24] for the copper atoms and 6-311+G(d) basis sets[23] for the others (denoted as B3LYP/6311A). The isotropic value of Me_4Si was 182.0 ppm. The maximum deviation of the GIAO ^{13}C chemical shift of 2-cyclohexenone from the experimental values[32] was 11.4 ppm, which indicates that the absolute value of the calculated chemical shift was not exact.

Results and Discussion

Energetics and pathway: Figure 1 shows the B3LYP/631A//B3LYP/321A energy profile of the reaction for the axial and equatorial pathways. The stationary points in the axial pathway will be denoted as ax (e.g. **TSccax**) and those in the equatorial pathway as eq (e.g. **TScceq**). In agreement with the experiments,[1–3] the axial product formation is favored at all stages of the reaction except in the product complex (**PD**). The structures of the stationary points are shown in schematic representation (Scheme 6), and in 3D pictures (Figure 3 for the axial attack pathway, and in the Supporting Information for the equatorial attack pathway). Figure 2 shows geometric parameters (a and b) and natural charges (c) for the representative stationary points in the axial pathway at the

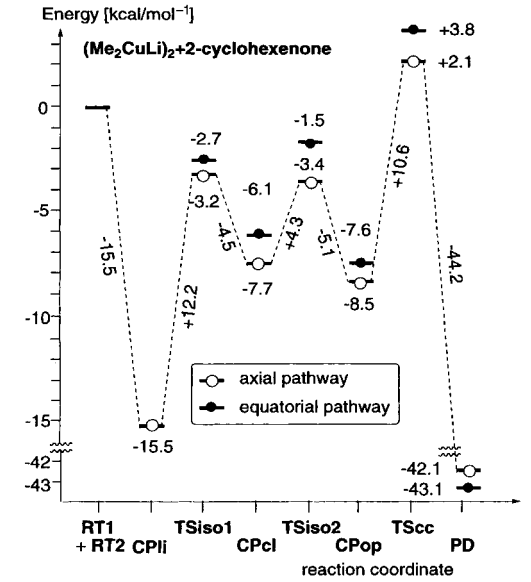

Figure 1. Energy changes in the conjugate addition of 2-cyclohexenone with $(Me_2CuLi)_2$ (B3LYP/631A//B3LYP/321A). Values given below the stationary structures are energy relative to reactants (**RT1**+**RT2**) in kcal mol^{-1} and values besides dashed lines are energy changes in kcal mol^{-1}. Bars with open circles are for "axial" attack and those with closed circles are for "equitorial" attack.

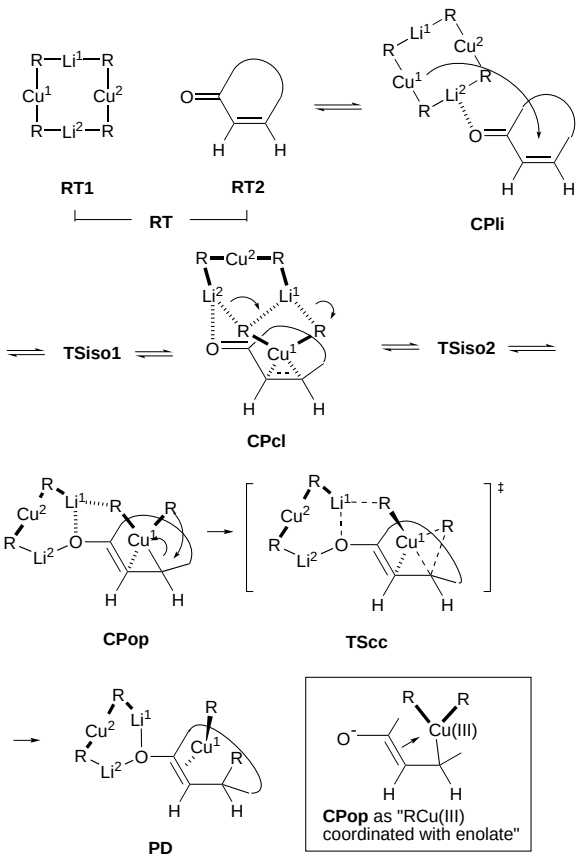

Scheme 6.

0947-6539/99/0505-1536 $ 17.50+.50/0 *Chem. Eur. J.* **1999**, *5*, No. 5

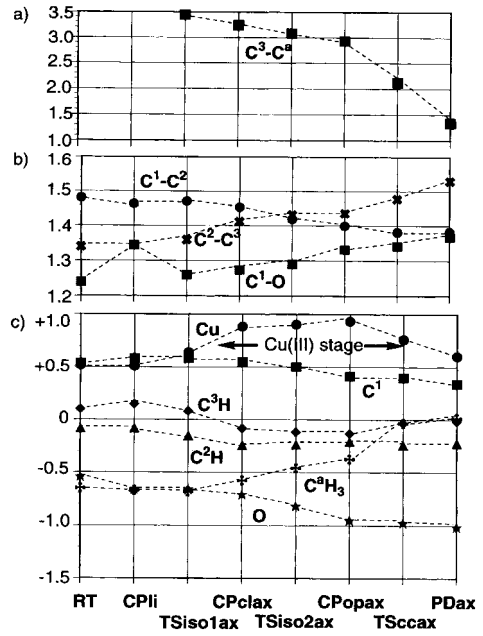

Figure 2. Change of a) C^3-C^a length in Å; b) representative atomic distances in Å; c) natural charges of representative atoms and groups in the axial pathway (B3LYP/631A//B3LYP/321A).

B3LYP/631A//B3LYP/321A level (and at the B3LYP/631A//B3LYP/631A level in parentheses). The energetics and structures of the cyclohexenone reaction are similar to those of the acrolein reaction reported earlier.[17]

As in the case of acrolein,[17] conjugate addition to cyclohexenone (**RT2**) under gas-phase conditions was found to take place in four stages, namely: oxygen/lithium complexation (**CPli**), olefin/copper closed complex formation (**CPclax**, **eq**), open complex formation (**CPopax**, **eq**), and product formation (**PDax**, **eq**). It was previously shown that **CPcl** having the pentacoordinated C^aH_3 group cannot directly go to **PD** without first achieving tetracoordination of the carbon atom as in **CPop.** The energy profile indicates that three energy barriers exist, olefin/copper π-bond formation (**TSiso1**, where the cuprate sits on one face of the olefin), cluster reorganization from closed to open complex (**TSiso2**), and C–C bond formation (**TScc**).[33] Note that the extremely large exothermicity of **CPli** formation (Figure 1 and Scheme 7) is the artifact of the lack of solvent. The formation

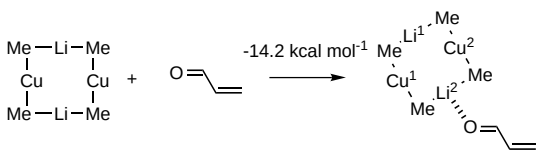

Scheme 7.

of **CPli** is simply a ligand–exchange process in solution. Indeed, as shown in Scheme 8, the ligand exchange between Me_2O and acrolein is almost thermoneutral. Under such conditions, **CPli** is just as stable as the starting materials. In solution, Li^1 must also be coordinated by a solvent molecule.[34, 35] Note that the lack of kinetic importance of the

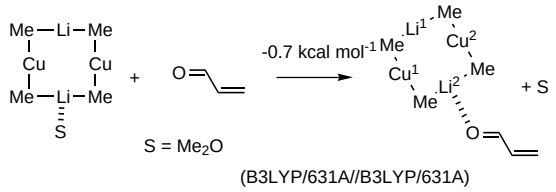

Scheme 8.

lithium/carbonyl complexation was also shown experimentally (cf. Scheme 4). It is also notable that solvent coordination on Li^2 in **CPcl** will significantly weaken the Li^2–oxygen (π-)coordination in this intermediate.

The last energy barrier (**TSccax**) represents the highest point on the potential energy surface of the reaction. This energy profile is consistent with experimental kinetics and kinetic isotope effects as discussed later.[36] The calculated energy barrier of about 11 kcal mol^{-1} (B3LYP/631A//B3LYP/321A) may become a few kcal mol^{-1} higher with a higher theoretical model (i.e., CCSD(T)[19, 37]). The product **PD** is a copper-complexed lithium enolate, and this structure probably reflects only part of the reality. If the cuprate is specifically Me_2CuLi, the MeCu product precipitates quantitatively as polymeric material, leaving pure lithium enolate.[38, 39]

As seen in the charge data shown in Figure 2c (B3LYP/631A//B3LYP/321A), two events are involved in the conjugate addition with respect to the electron flow between cuprate and cyclohexenone (also previously found for acrolein).[17] At the first stage, electron donation from the copper atom to the enone generates a Cu^{III} state, which reverts to a Cu^{I} state in the second stage (see box in Scheme 6 for a schematic representation of the Cu^{III} intermediate.) In the first event from **RT1** to **CPopax**, the electron density at C^3H_2 and carbonyl oxygen increases, and that at Cu^1 decreases because of back-donation from Cu^1 to 2-cyclohexenone. The negative charge on the oxygen atom increased to -0.95 e during conversion. In conjunction with this change, **CPopax** already shows the enolate character (long C^1—O and short C^1—C^2) (Figure 3), and the C^2 enolate carbon acts as a stabilizing basic ligand to the Cu^{III} atom.[40]

Some details of the stationary points are described below for the axial attack path (Figure 3). The complex **CPclax** is a two-point binding complex, wherein the dimer and the enone are bound together through Cu^1 and Li^2 (front view in Figure 3). The $C^a-Cu^1-C^b$ bond is bent and the Cu^1 atom is tightly bound to the olefin. Thus, the four Cu–C bonds on Cu^1 are of nearly equal length (2.032–2.085 Å), and the Cu^1 atom has a near square planar geometry, that is, a geometry conforming to the d^8 Cu^{III} formalism.[41, 42] These structural changes coincide with electron donation from copper to enone (cf. Cu^1 and C^3H in Figure 2c). The olefinic bond (1.412 Å) is elongated halfway from the enone (**RT2**, 1.340 Å) to the product (**PDax**, 1.530 Å), which is consistent with the Krause results of the reported ^{13}C NMR spin coupling data.[14]

In **CPopax**, the Li^2 atom is totally detached from the C^b methyl group. This bond reorganization frees the C^a methyl group from lithium coordination. Being electrostatic in nature, the bond between the dicoordinated lithium atom

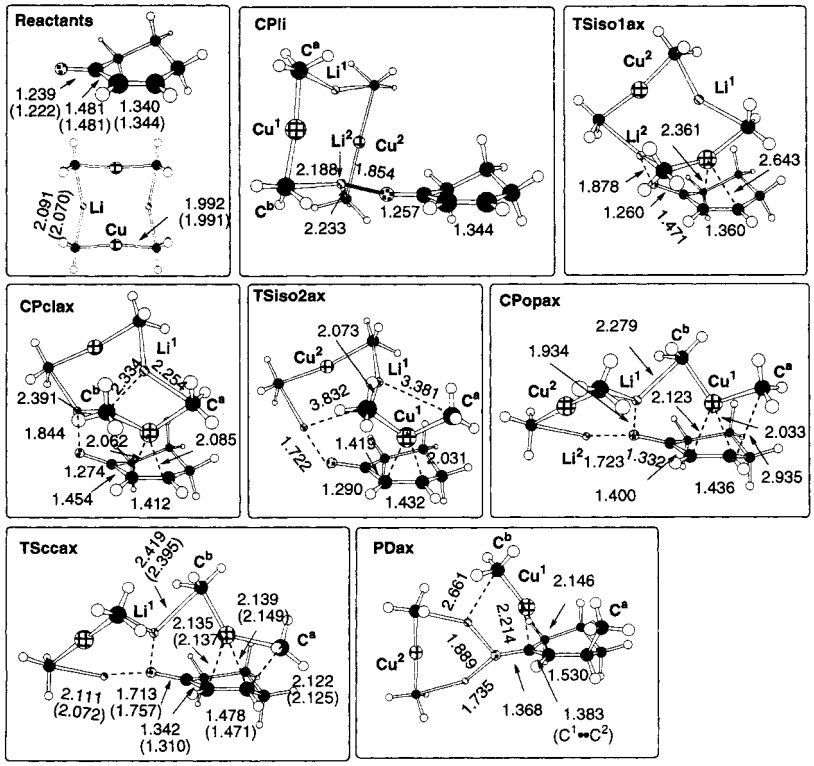

Figure 3. Reactants, intermediates, and TSs in the conjugate addition of $(Me_2CuLi)_2$ to 2-cyclohexenone. Bond lengths [Å] are at the B3LYP/321A level (those in parentheses are at the B3LYP/631A level). Values of imaginary frequencies of **TSiso1ax**, **TSiso2ax**, and **TSccax** are 117.5*i*, 48.9*i*, and 323.7*i* cm^{-1}, respectively. Total energies of **RT1** and **RT2** at the B3LYP/631A//B3LYP/321A level are −3455.479138 and −308.665269 hartrees, respectively.

and the pentacoordinated alkyl group in cuprate in solution is short, but is not a static bond.[43]

The major event in **TSccax** that directly follows **CPopax** is the C^3–C^a bond formation (see also Figure 2a). In addition, the Cu^1 atom is datively coordinated by the C^1=C^2 π bond of the enolate.[17, 44] The formation of the product **PD** is a highly exothermic process.

The issue of axial/equatorial preference: The calculations show that the equatorial pathway is consistently 0.5–1.7 kcal mol^{-1} higher in energy than the axial pathway throughout the reaction course except in **PD** (Figure 1). The origin of the energy difference is examined in this section.

Since the Curtin–Hammett boundary condition is satisfied, the energy profile indicates that the diastereofacial selectivity is determined at the last C–C bond-forming step. The axial preference amounts to 1.61 kcal mol^{-1} (B3LYP/631A//B3LYP/631A level, translating to a 98:2 ratio at −70 °C), which is a reasonable value (Scheme 1). The axial preference at the MP2/631A//B3LYP/631A level is 2.47 kcal mol^{-1}, and that at the MP4SDQ level (see section on Chemical Models and Computational Details) is 1.81 kcal mol^{-1}.

To see where this energy difference comes from, we removed the organometallic part from **TScc**, extracted the cyclohexenone + C^aH_3 moiety, and generated structures **G** and **H** shown in Figure 4. The axial/equatorial energy difference for these models was 2.1 kcal mol^{-1}. Thus, most of the axial preference comes from the cyclohexenone + C^aH_3 part, since the cluster moiety is flexible enough not to contribute much to the diastereomeric energy difference. This energy difference can be related conceptually to the difference (+6.3 kcal mol^{-1}) between an axially substituted chair cyclohexane **I** and an equatorially substituted boat cyclohexane **J**. Note that the structural details such as the elongated C^3–C^aH_3 bonds in **G** and **I** are important for them to exist as different entities, since simple structure optimization from **G** and **I** led to the same 3-methylcyclohexanone enolate. It is important to note also that the axial/equatorial difference decreases to 0.08 kcal mol^{-1} (equatorial preference) if only the cyclohexenone part (i.e. without C^aH_3) is extracted from **TScc**. The above analysis also accounts for puzzling cases such as Scheme 1, wherein the diastereoselectivity appears to reflect the product stability. Clearly, the angular methyl

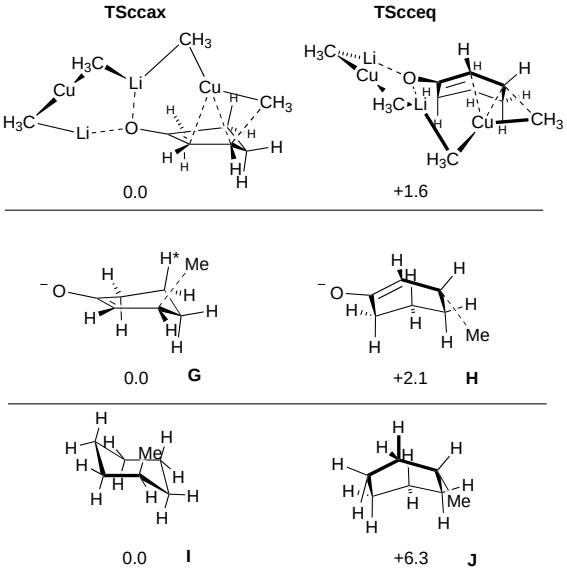

Figure 4. Origin of the energy difference in axial and equatorial attacks (B3LYP/631A//B3LYP/631A). The energies of the structures on the right relative to those on the left are in kcal mol^{-1}.

group in the steroidal CD ring system in Scheme 1, which is equivalent to substitution of H* in **TSccax** (and **G**), destabilizes the axial TS because of 1,3-diaxial interaction. Details will be discussed in the Conclusion section.

Comparison of TSs between acrolein and cyclohexenone reactions: In this section, we will compare the TSs of rate-

0947-6539/99/0505-1538 $ 17.50+.50/0 *Chem. Eur. J.* **1999**, *5*, No. 5

limiting C–C bond formation for acrolein and cyclohexenone reactions. This comparison of structural parameters revealed rather remarkable insensitivity of the TS geometry to the substrate. Since the TS structure is also rather insensitive to the nature of the cuprate model (i.e. $Me_2CuLi \cdot LiI$ and $(Me_2CuLi)_2$),[17] we expect that realistic systems will be easily modeled by a combined MO/MM method.[45]

Thus, we compared the partial structures for C^1, C^2, C^3 and the carbonyl oxygen between acrolein and cyclohexenone, as shown in Figure 5 (both at the B3LYP/631A level). The O–C^1–C^2–C^3 angle with acrolein is $-165.0°$, while it is $-167.6°$

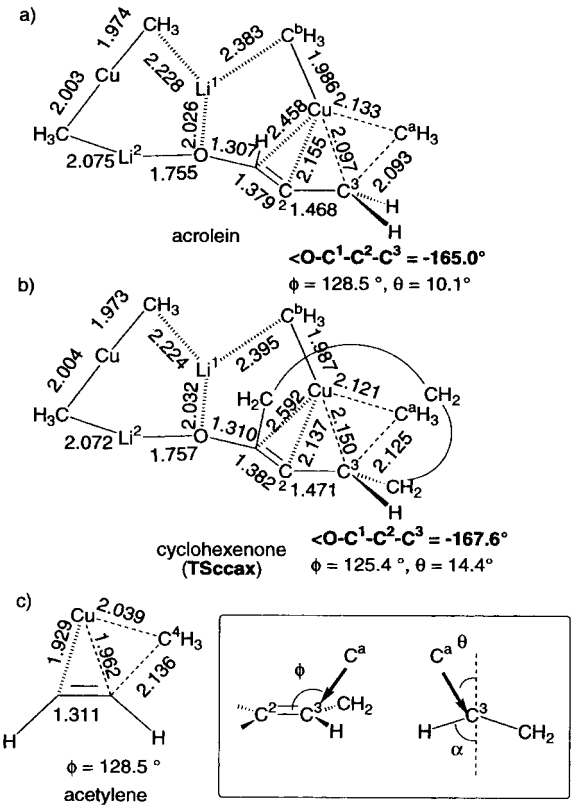

Figure 5. Differences of geometries of TSs in the a) conjugate addition of acrolein; b) conjugate addition of 2-cyclohexenone with $(Me_2CuLi)_2$; and c) addition of acetylene with MeCu (B3LYP/631A).

with cyclohexenone. This constancy of angle must be caused by the electronic features of Cu^{III} reductive elimination, namely, dative coordination of the enolate olefin to Cu^{III} and the enolate nature of O–C^1–C^2 moiety. In addition, the trajectory of the C^aH_3 group was similar in the two cases. An angle θ was defined as the deviation of the incoming C^a from the normal plane (defined as a plane dividing the two planes made by the olefinic C^2=C^3 bond, CH_2, and H).[46] The angle θ is 10.1° for acrolein, and 14.4° and 16.8° for **TSccax** and **TScceq**. The incoming angle ϕ is 128.5° or 123.9°. It is interesting to note that ϕ is also 128.5° in the TS of MeCu addition to acetylene,[19] which further illustrates the general persistence of the Bürgi–Dunitz principle.[47]

Having obtained the structures of intermediates and transition states, we will next compare their calculated physical properties with the experimental data.

^{13}C NMR chemical shifts: Although experimental NMR measurements of the intermediates of conjugate addition provided valuable information on the structures occupied by the NMR-measurable nuclei, they offered no molecular pictures of the whole structure. Comparison of computational and experimental ^{13}C NMR chemical shift values offers a valuable reference point for probing the nature of intermediates in the reaction pathway.[48]

Unlike highly reactive 2-cyclohexenone itself (with which equilibrium concentrations of the intermediates are too reactive to be detected), β,β-substituted α,β-enones such as 10-methyl-$\Delta^{1,9}$-2-octalone (Scheme 9)[12] and 2,2,5-trimethylhex-4-en-3-one (Scheme 10)[13] are sterically hindered around

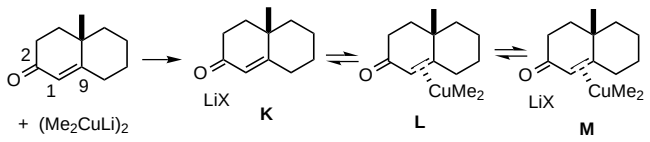

Scheme 9.

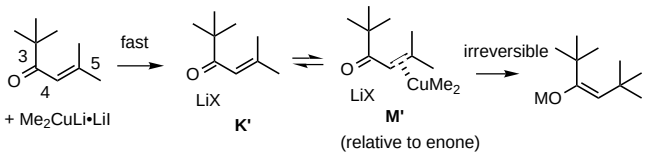

Scheme 10.

the olefinic region, and hence unreactive enough to allow detection of cuprate complexes. Thus, mixing $(Me_2CuLi)_2$ with the former enone in $[D_{10}]$diethyl ether at $-78\,°C$ has been reported to result in quantitative conversion of the enone to a mixture of species considered to be lithium/carbonyl (**K**), copper/olefin (**L**), and lithium-coordinated copper/olefin (**M**) complexes (Scheme 9), and mixing $Me_2CuLi \cdot LiI$ with the latter enone quantitatively afforded two complexes **K′** and **M′** (Scheme 10). Notably, lithium carbonyl complex **K′** did not produce the product, and only **M′** went directly to the product at $-60\,°C$. This is consistent with the Smith/Krauss picture (Scheme 4).[9] The intermediates such as **K**, **L**, and **M** probably correspond to **CPli**, **CPcl**, and **CPop**, respectively.

Spectral comparison of the starting enone with the enone/cuprate complex was made for two real enones (Figure 6a–d) and the present theoretical models (Figure 6e, f). The experimental spectra of the complex and the theoretical spectra calculated for **CPop** showed good agreement, indicating that **K** and **K′** are likely to be the **CPop** species. This assignment was consistent with the experimental and theoretical conclusions (vide infra) that these copper/olefin complexes were direct precursors to the product. Thus, the spectral characteristics of **K** and **K′** compared with the starting enones (Figure 6a, b and 6c, d, respectively) were such that the carbonyl carbon underwent a small upfield shift (7–9 ppm) and the olefinic carbon a large upfield shift (75–95 ppm). A similar upfield shift was calculated for **CPop.** From the charge and structure analysis (vide supra), the upfield shift of the

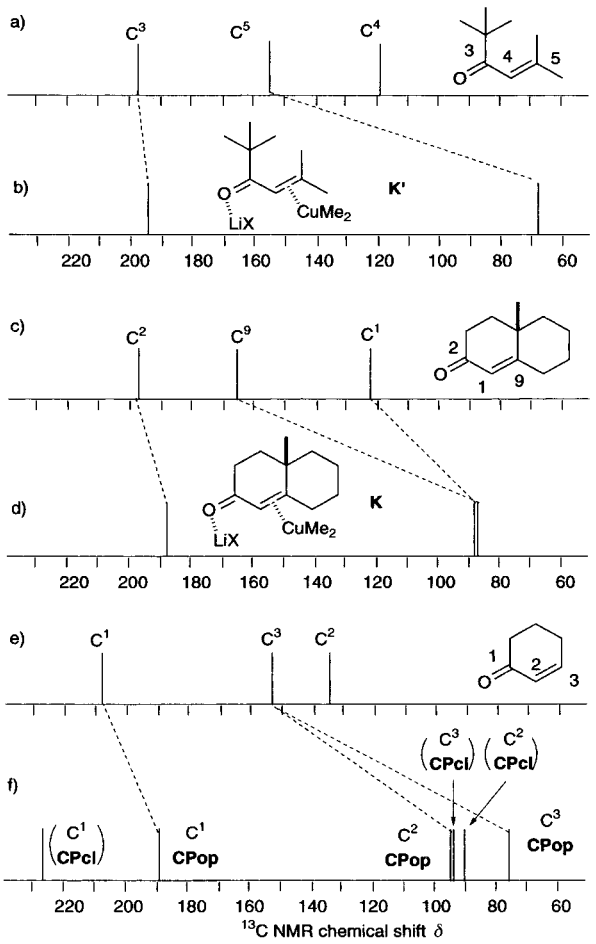

Figure 6. Experimental ^{13}C NMR chemical shift values for: a) 2,2,5-trimethylhex-4-en-3-one; b) its 1-complex with $Me_2CuLi \cdot LiI$ in $[D_{10}]$diethyl ether; c) 10-methyl-$\Delta^{1,9}$-2-octalone; and d) its π complexes with $(Me_2CuLi)_2$ in $[D_{10}]$diethyl ether, and calculated ^{13}C NMR chemical shift values (B3LYP/6311A//B3LYP/321A) for: e) 2-cyclohexenone (axial pathway); and f) 1-complexes of 2-cyclohexenone with $(Me_2CuLi)_2$.

carbonyl carbon was due to charge build-up, and that of the olefinic carbons was due to sp^2 to sp^3 rehybridization. The magnitude of the upfield shift of the carbonyl carbon in the experiments was smaller than the calculated data (6b, d vs. 6f); this may be due to the small equilibrium contribution of **CPcl**, which has a downfield shift (owing to electrophilic coordination of Li^2).

Kinetic isotope effects: Experimental KIE investigations provide valuable information on the nature of the transition state. Recent experimental studies[16] on the conjugate addition of $Bu_2CuLi \cdot LiI$ and $Bu_2CuCNLi$ (Table 1, entries 1 and 2) showed a large KIE for the two carbon atoms associated with the σ-bond formation, C^3 and C^a. The KIE values for the latter carbon atom depend on the cuprate structures (1.014 and 1.020). Other carbon atoms on the enone showed KIE values indicative of small changes of bonding state between the

Table 1. Experimental KIE and theoretical KIE calculated for **TSccax** against **CPopax** with the Bigeleisen–Mayer equation with Wigner tunnel correction (B3LYP/321A).

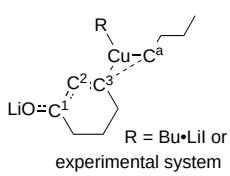

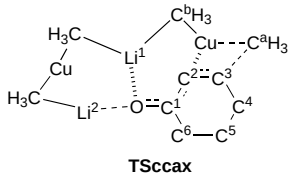

Entry	C^1	C^2	C^3	C^4	C^5	C^6	C^a	
1	1.002	1.005	1.023	0.998	1.005	1.000	1.014	exp $Bu_2CuLi \cdot LiI$
2	–	–	–	–	–	–	1.020	exp $Bu_2CuCNLi$
3	0.999	1.006	1.018	0.997	1.000	1.000	1.032	calcd

rate-limiting steps and the starting material. The identity of this starting material was shown, by NMR studies and energy profile, to be the copper/olefin complex **CPop** that exists as a predominant stable intermediate in solution. Calculation of the KIE of **TSccax** based on **CPopax** showed good agreement with the experimental values, especially for the enone carbon atoms including C^3 (Table 1, entry 3). The KIE value for the incoming methyl group (1.032) was slightly larger than the experimental value (1.014–1.020) obtained for butyl cuprates, and this discrepancy may have arisen from experimental and theoretical factors (e.g. theoretical method, model, difference of the cuprate reactants).[49, 50]

Conclusion

In the present studies, we have examined two diastereomeric pathways of the conjugate addition of $(Me_2CuLi)_2$ to 2-cyclohexenone in the gas phase and determined intermediates and TSs lying on the pathway leading to the conjugate addition product. The studies have provided the first solid correlation between the physicochemical data and the concrete molecular structures.

Among various models suggested thus far in the literature, the present models are the closest to the experimental examples, and provide the first molecular picture of the nature of the diastereoselectivity of the cuprate addition. Translation of preferred **TSccax** in Figure 4 into the archetypal experimental case of Scheme 2b and Scheme 3 generates a model for axial attack **P** (Scheme 11. The 1,2-diastereoselectivity in Scheme 2a was probably due to the axial attack **Q** (Scheme 12) where the 4-methyl group is in the axial position owing to the presence of the flat sp^2 carbons in the ring. When there is steric hindrance disfavoring the axial attack, as in Scheme 1, the reaction may take place via a boat TS **S** (i.e. **TScceq**) rather than a chair TS **R** (Scheme 13).

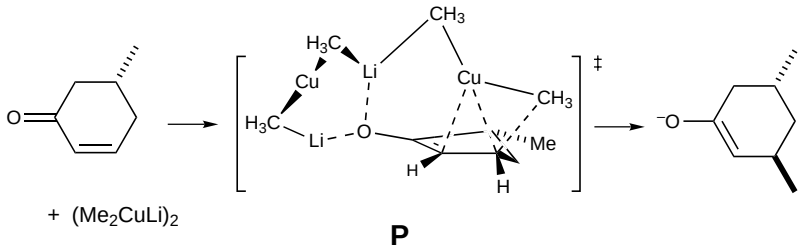

Scheme 11.

0947-6539/99/0505-1540 $ 17.50+.50/0 Chem. Eur. J. 1999, 5, No. 5

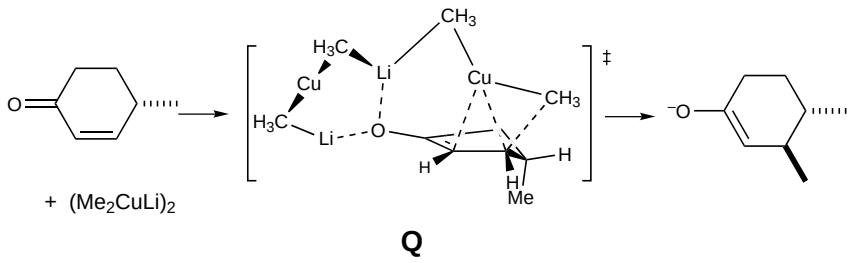

Scheme 12.

The present studies have shown that the intermediate similar to **CPop** directly goes to the transition state leading to the conjugate adduct (the box in Scheme 14). The stereoselectivity of the addition reflects the conformation energy of the TS, having little to do with the starting material (cyclohexenone), despite the high exothermicity of the reaction. This was another illustration of the inappropriateness of straightforward application of Hammond's postulate to organometallic reactions.[51] Given the known fractional behavior of lithium cuprate in solution,[43a, b] we can now draw the following scheme for the pathway of conjugate addition (Scheme 14; solvent participation was neglected for clarity). Thus, one can consider an extreme case of the associative pathway (top left) leading to **CPop** as suggested by the gas-phase calculations, as well as a dissociative process (bottom left) involving prior opening of the cuprate cluster (**N**) which goes directly to **CPop** without going through **CPli** or **CPcl**. Linear polymers of lithium cuprates found in crystals (including the higher-order cuprate)[43c–e, 52] will also serve as the source of the open complex in solution. A copper/olefin one-point binding complex **O** may also lie on the pathway. The overall energetic surface was rather flat, with the highest point at **TScc**, which was also the face-selectivity-determining step. The effect of Me_3SiCl in accelerating the conjugate addition that we first reported in 1984[53, 54] was probably to lower the energy of this final C–C bond-forming step by reducing the electron-donating power of the lithium enolate moiety by in-situ conversion to the corresponding enol silyl ether (bottom right).

On the basis of this information on the face-selectivity step, we consider that the role of effective chiral ligands reported recently[55] is to selectively accelerate reductive elimination of the **CPop** intermediate, most likely through complexation of

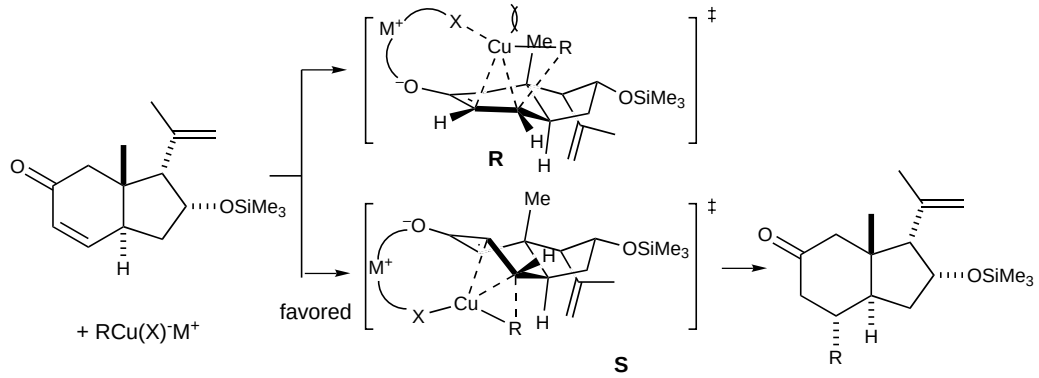

Scheme 13.

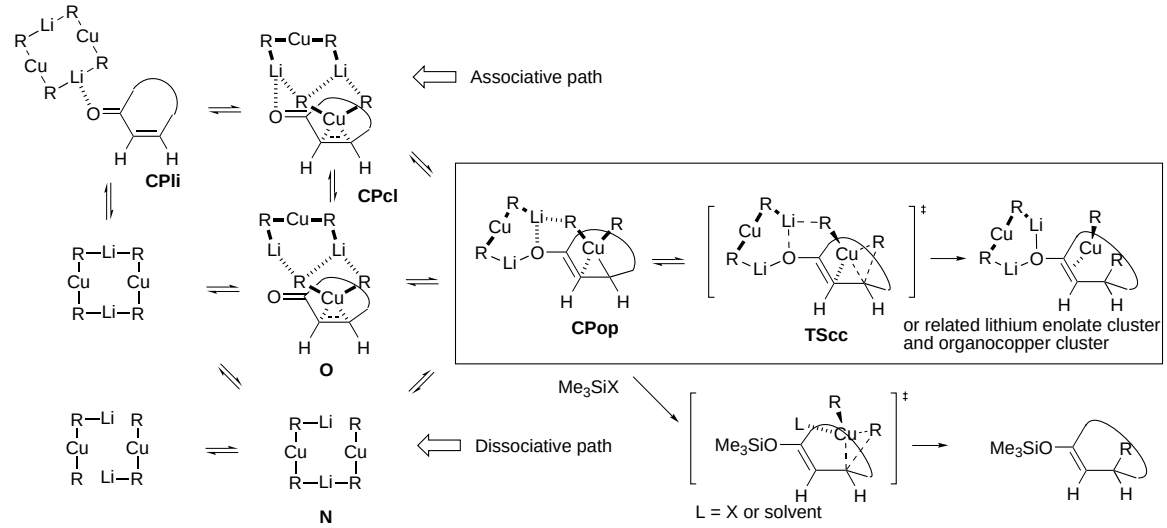

Scheme 14.

the phosphorus moiety of the ligand to the Cu^{III} atom in **TScc**. Note that this view is quite different from the prevailing views on enantiofacially selective conjugate addition that focus on the copper/olefin 1-complexation stage (e.g. **CPcl**) as the crucial face-selective step (Scheme 15).[56]

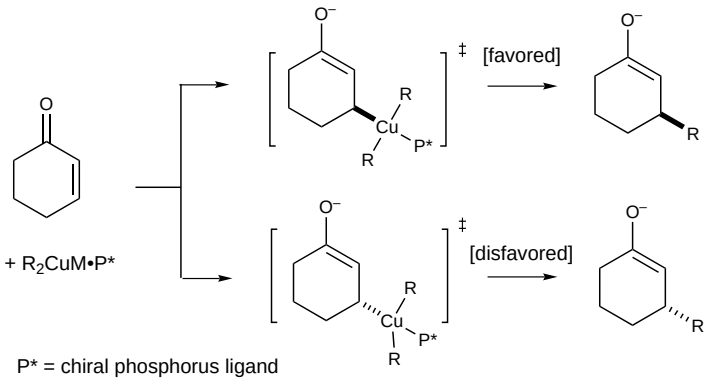

Scheme 15.

Supporting information: Supporting information for this article is available on the WWW under http://www.wiley-vch.de/home/chemistry/ or from the authors, who can supply a directory; it contains Cartesian coordinates of the stationary points, representative frequencies of TSs, and 3D structures on the stationary points on the equatorial attack pathway in the conjugate addition of 2-cyclohexenone with $(Me_2CuLi)_2$ at the B3LYP/321A level.

Acknowledgments

We thank Prof. H. Yamataka for helpful discussions. This work was supported by a Grant-in-Aid for Scientific Research on Priority Areas (No. 283, Innovative Synthetic Reactions) from Monbusho, Japan. Generous allotment of computational time from the Institute for Molecular Science is gratefully acknowledged. S.M. thanks JSPS for a pre- and postdoctoral fellowship.

[1] See, for example: a) G. Stork, R. A. Kretchmer, R. H. Schlessinger, *J. Am. Chem. Soc.* **1968**, *90*, 1647–1648; b) C. H. Heathcock, E. F. Kleinman, E. S. Binkley, *J. Am. Chem. Soc.* **1978**, *100*, 8036–8037; c) G. H. Posner, *Organic Reactions* **1972**, *19*, 1–113; J. A. Kozlowski, *Comprehensive Organic Synthesis*, *Vol. 4* (Eds.: B. M. Trost, I. Fleming), Pergamon, Oxford, **1991**, pp. 169–198; B. H. Lipshutz, S. Sengupta, *Organic Reactions* **1992**, *41*, 135–631.

[2] Y. Horiguchi, E. Nakamura, I. Kuwajima, *J. Am. Chem. Soc.* **1989**, *111*, 6257–6265.

[3] H. O. House, W. F. Fischer, Jr., *J. Org. Chem*, **1968**, *33*, 949–956.

[4] N.-T. Luong-Thi, H. Revière, *C. R. Acad. Sci. Ser. C.* **1968**, *267*, 776–778; see G. Hareau-Vittini, S. Hikichi, F. Sato, *Angew. Chem.* **1998**, *110*, 2221–2223; *Angew. Chem. Int. Ed.* **1998**, *37*, 2099–2101.

[5] See P. Chamberlain, G. H. Whitham, *J. Chem. Soc. Perkin Trans II* **1972**, 130–135; see also: T. A. Blumenkopf, C. H. Heathcock, *J. Am. Chem. Soc.* **1983**, *105*, 2354–2358; T. R. Hoye, A. S. Magee, R. E. Rosen, *J. Org. Chem.* **1984**, *49*, 3224–3226.

[6] E. J. Corey, F. J. Hannon, *Tetrahedron Lett.* **1990**, *31*, 1393–1396; see P. Perlmutter, *Conjugate Addition Reactions in Organic Synthesis*, Pergamon, Oxford, **1992**, Chapter 1, pp. 25–27.

[7] E. L. Eliel, S. H. Wilen, L. N. Mander, *Stereochemistry of Organic Compounds*, Wiley, **1993**, pp. 890.

[8] B. E. Rossiter, M. Eguchi, G. Miao, N. M. Swingle, A. E. Hernández, V. Vickers, E. Fluckiger, R. G. Peterson, K. V. Reddy, *Tetrahedron* **1993**, *49*, 965–986.

[9] S. R. Krauss, S. G. Smith, *J. Am. Chem. Soc.* **1981**, *103*, 141–148.

[10] The studies also indicated that each step is not directly affected by the reduction potential of the enone (contrary to the prior House qualitative analysis: H. O. House, *Acc. Chem. Res.* **1976**, *9*, 59–67).

[11] a) G. Hallnemo, T. Olsson, C. Ullenius, *J. Organomet. Chem.* **1984**, *265*, C22-C24; b) G. Hallnemo, T. Olsson, C. Ullenius, *J. Organomet. Chem.* **1985**, *282*, 133–144; c) B. Christenson, G. Hallnemo, C. Ullenius, *Chem. Script.* **1987**, *27*, 511–512; d) C. Ullenius, B. Christenson, *Pure Appl. Chem*. **1988**, *60*, 57–64.

[12] S. H. Bertz, R. A. J. Smith, *J. Am. Chem. Soc.* **1989**, *111*, 8276–8277.

[13] A. S. Vellekoop, R. A. J. Smith, *J. Am. Chem. Soc.* **1994**, *116*, 2902–2913.

[14] N. Krause, R. Wagner, A. Gerold, *J. Am. Chem. Soc.* **1994**, *116*, 381–382.

[15] The PRDDO calculated π complex of acrolein was carried out for Me_3CuLi_2. J. P. Snyder, G. E. Tipsword, D. J. Splanger, *J. Am. Chem. Soc.* **1992**, *114*, 1507–1510.

[16] D. E. Frantz, D. A. Singleton, J. P. Snyder, *J. Am. Chem. Soc.* **1997**, *119*, 3383–3384.

[17] E. Nakamura, S. Mori, K. Morokuma, *J. Am. Chem. Soc.* **1997**, *119*, 4900–4910 (3D pictures and coordinates are available on: http://www.chem.s.u-tokyo.ac.jp/~common/Theo/Cj1/title); see also E. Nakamura, S. Mori, K. Morokuma, *J. Am. Chem. Soc.* **1998**, *120*, 8273–8274 (3D pictures and coordinates are available on: http://www.chem.s.u-tokyo.ac.jp/~common/Theo/Sn1/title).

[18] See A. Bernardi, A. M. Capelli, C. Gennari, C. J. Scolastico, *Tetrahedron: Asymmetry* **1990**, *1*, 21–32.

[19] E. Nakamura, S. Mori, M. Nakamura, K. Morokuma, *J. Am. Chem. Soc.* **1997**, *119*, 4887–4899 (3D pictures and coordinates are available on: http://www.chem.s.u-tokyo.ac.jp/~common/Theo/Cb/title); S. Mori, E. Nakamura, *J. Mol. Struct (Theochem)*, in press.

[20] Gaussian 94, Revision E.2, M. J. Frisch, G. W. Trucks, H. B. Schlegel, P. M. W. Gill, B. G. Johnson, M. A. Robb, J. R. Cheeseman, T. Keith, G. A. Petersson, J. A. Montgomery, K. Raghavachari, M. A. Al-Laham, V. G. Zakrzewski, J. V. Ortiz, J. B. Foresman, J. Cioslowski, B. B. Stefanov, A. Nanayakkara, M. Challacombe, C. Y. Peng, P. Y. Ayala, W. Chen, M. W. Wong, J. L. Andres, E. S. Replogle, R. Gomperts, R. L. Martin, D. J. Fox, J. S. Binkley, D. J. Defrees, J. Baker, J. P. Stewart, M. Head-Gordon, C. Gonzalez, and J. A. Pople, Gaussian, Pittsburgh PA, **1995**.

[21] A. D. Becke, *J. Chem. Phys.* **1993**, *98*, 5648–5652; C. Lee, W. Yang, R. G. Parr, *Phys. Rev. B* **1988**, *37*, 785–789.

[22] There was found to be little biradical character in the complexes and the TSs at the UB3LYP/631A level. See E. Goldstein, B. Beno, K. N. Houk, *J. Am. Chem. Soc.* **1996**, *118*, 6036–6043.

[23] W. J. Hehre, L. Radom, P. von R. Schleyer, J. A. Pople, *Ab Initio Molecular Orbital Theory*, Wiley, New York, **1986**, references cited therein.

[24] A. Schäfer, H. Horn, R. Ahlrichs, *J. Chem. Phys.* **1992**, 97, 2571–2577.

[25] A. E. Reed, L. A. Curtiss, F. Weinhold, *Chem. Rev.* **1988**, *88*, 899–926. NBO Version 3.1 in Gaussian 94 package implemented by E. D. Glendening, A. E. Reed, J. E. Carpenter, F. Weinhold.

[26] Structural comparison between the 321A and the 631A basis sets for the acrolein case[17] and for **TScxax** and **TScceq** (see Figure 5b) indicated that the B3LYP/321A structures show reasonable agreement with the B3LYP/631A structures (<5% difference as to bond lengths). The 321A basis set, however, systematically overestimated the lithium–oxygen interaction energy because basis set superposition error overestimates the interaction between lithium and oxygen.

[27] Energy differences of equatorial/axial isomers of methylcyclohexane, which is a case related closely to ours, are 2.1 kcal mol^{-1} at the B3LYP/6-31G* level, compared to the experimental value of 1.8 kcal mol^{-1}: W. J. Hehre, *Practical Strategies for Electronic Structure Calculations*, Chapter 6, Wavefunction Inc., **1995**.

[28] L. Melander, W. H. Saunders, Jr., *Reaction Rates of Isotopic Molecules*, Wiley, Chichester, New York, **1980**.

[29] J. Bigeleisen, M. G. Mayer, *J. Chem. Phys.* **1947**, *15*, 261–267; J. Bigeleisen, M. Wolfsberg, *Adv. Chem. Phys.* **1958**, *1*, 15–76; see also: H. Yamataka, S. Nagase, *J. Am. Chem. Soc.* **1998**, *120*, 7530–7536.

[30] A. P. Scott, L. Radom, *J. Phys. Chem.* **1996**, *100*, 16502–16513

[31] R. Ditchfield, *Mol. Phys.* **1974**, 27, 789–807. J. R. Cheeseman, G. W. Trucks, T. A. Keith, M. J. Frisch, *J. Chem. Phys.* **1996**, 104, 5497–5509.

[32] G. C. Levy, R. L. Lichter, G. L. Nelson, *^{13}Carbon Nuclear Magnetic Resonance Spectroscopy, 2nd ed.*, Wiley, New York, **1980**.

0947-6539/99/0505-1542 $ 17.50+.50/0 *Chem. Eur. J.* **1999**, *5*, No. 5

[33] See: a) M. P. Bernstein, D. B. Collum, *J. Am. Chem. Soc.* **1993**, *115*, 789–790; b) P. G. Willard, Q.-Y. Liu, *J. Am. Chem. Soc.* **1993**, *115*, 3380–3381; c) M. Nakamura, E. Nakamura, N. Koga, K. Morokuma, *J. Am. Chem. Soc.* **1993**, *115*, 11016–11017; M. Nakamura, E. Nakamura, N. Koga, K. Morokuma, *J. Chem. Soc. Faraday Trans.* **1994**, *90*, 1789–1798; S. Mori, B. H. Kim, M. Nakamura, E. Nakamura, *Chem. Lett.* **1997**, 1079–1080 (3D pictures and coordinates are available on: http://www.chem.s.u-tokyo.ac.jp/~common/Theo/Cl2/title); d) M. Yamakawa, R. Noyori, *J. Am. Chem. Soc.* **1995**. *117*, 6327–6335.

[34] The lithium atom in $[R_2CuLi]_2$ in crystals is typically solvated with one solvent molecule on each lithium atom: a) G. van Koten, J. T. B. H. Jastrzebski, F. Muller, C. H. Stam, *J. Am. Chem. Soc.* **1985**, *107*, 697–698; b) M. M. Olmstead, P. P. Power, *Organometallics* **1990**, *9*, 1720–1722.

[35] Solvation lessens the energy difference caused by the change of coordination number on a lithium atom such as that occurring between **CP** and **TS**: M. T. Rodgers, P. B. Armentrout, *J. Phys. Chem. A.* **1997**, *101*, 1238–1249.

[36] Compared with the energetics for acrolein in ref. [16], the stationary points after **CPop**, wherein the ketone is enolized, are consistently higher in energy by several kcal mol^{-1} than those before, where the ketone largely retains its C=O structure. This difference may be due to the stability of aldehyde enolate over ketone enolate (electron-donating substituents destabilize enolate anion: c.f. F. G. Bordwell, F. Cornforth, *J. Org. Chem.* **1978**, *43*, 1763–1768).

[37] G. E. Scuseria, A. C. Scheiner, T. J. Lee, J. E. Rice, H. F. Schaefer, III, *J. Chem. Phys.* **1987**, 86, 2881–2890; J. A. Pople, M. Head-Gordon, K. Raghavachari, *J. Chem. Phys.* **1987**, *87*, 5968–5975.

[38] H. O. House, J. M. Wilkins, *J. Org. Chem.* **1976**, *41*, 4031–4032.

[39] H. O. House, J. M. Wilkins, *J. Org. Chem.* **1978**, *43*, 2443–2454.

[40] See a) A. E. Dorigo, J. Wanner, P. von R. Schleyer, *Angew. Chem.* **1995**, *107*, 492–494; *Angew. Chem. Int. Ed. Engl.* **1995**, *34*, 476–478; b) J. P. Snyder, *J. Am. Chem. Soc.* **1995**, *117*, 11025–11026.

[41] Standard inorganic convention utilizes formal charge on metals, knowing that that the charge on the center metal of an organo-transition metal is generally less positive than the formal charge (e.g. Cu is ca. +1 in R_3Cu^{III}). This view was recently challenged: J. P. Snyder, *Angew. Chem.* **1995**, *107*, 112; *Angew. Chem. Int. Ed. Engl.* **1995**, *34*, 80–81; M. Kaupp, H. G. von Schnering, *Angew. Chem.* **1995**, *107*, 1076; *Angew. Chem. Int. Ed. Engl.* **1995**, *34*, 986. J. P. Snyder, *Angew. Chem.* **1995**, *107*, 1076; *Angew. Chem. Int. Ed. Engl.* **1995**, *34*, 986–987.

[42] For X-ray crystal structures of organocopper(III) compounds, see: M. A. Willert-Porada, D. J. Burton, N. C. Baenziger, *J. Chem. Soc. Chem. Commun.* **1989**, 1633–1634; D. Neumann, T. Roy, K.-F. Tebbe, W. Crump, *Angew. Chem.* **1993**, *105*, 1555; *Angew. Chem. Int. Ed. Engl.* **1993**, *32*, 1482–1483; R. Eujen, B. Hoge, D. J. Brauer, *J. Organomet. Chem.* **1996**, *519*, 7–20.

[43] a) T. A. Mobley, F. Müller, S. Berger, *J. Am. Chem. Soc.* **1998**, *120*, 1333–1334; b) H. Huang, C. H. Liang, J. E. Penner-Hang, *Angew. Chem.* **1998**, *110*, 1628–1630; *Angew. Chem. Int. Ed.* **1998**, *37*, 1564–1566; c) G. Boche, F. Bosold, M. Marsch, K. Harms, *Angew. Chem.* **1998**, *110*, 1779–1781; *Angew. Chem. Int. Ed.* **1998**, *37*, 1684–1686; d) C.-S. Hwang, P. P. Power, *J. Am. Chem. Soc.* **1998**, *120*, 6409–6410; e) C. M. P. Kronenburg, J. T. B. H. Jastrzebski, A. L. Spek, G. van Koten, *J. Am. Chem. Soc.* **1998**, *120*, 9688–9689.

[44] See a) G. Hallnemo, C. Ullenius, C. *Tetrahedron* **1983**, *39*, 1621–1625; b) C. L. Kingsbury, R. A. J. Smith, *J. Org. Chem.* **1997**, *62*, 4629–4634; C. L. Kingsbury, R. A. J. Smith, *J. Org. Chem.* **1997**, *62*, 7637–7643.

[45] F. Maseras, K. Morokuma, *J. Comput. Chem.* **1995**, *16*, 1170; T. Matsubara, F. Maseras, N. Koga, K. Morokuma, *J. Phys. Chem.* **1996**, *100*, 2573–2580. ONIOM and IMOMM methods are implemented in the Gaussian 98 program.

[46] E. P. Lodge, C. H. Heathcock, *J. Am. Chem. Soc.* **1987**, *107*, 2819.

[47] H. B. Bürgi, J. D. Dunitz, J. M. Lehn, G. Wipff, *Tetrahedron* **1974**, *30*, 1563–1572; H. B. Bürgi, J. D. Dunitz, *Acc. Chem. Res.* **1983**, *16*, 153–161.

[48] ^{13}C GIAO chemical shifts (B3LYP/6311A//B3LYP/321A) on C^1, C^2, and C^3, respectively: a) 2-cyclohexenone $\delta = 208.5$, 135.4, 154.4; b) **CPcl** $\delta = 227.2$, 90.5, 93.4; c) **CPop** $\delta = 189.2$, 94.9, 75.8.

[49] The basic set dependence (B3LYP/321A vs. B3LYP/631A), Wigner tunneling effects on carbon KIEs, and effects of cuprate structures (i.e., Me_2CuLi, $Me_2CuLi \cdot LiCl$, $(Me_2CuLi)_2$, $[Me_2CuLi(H_2O)]_2$, MeEtCuLi) were found to be much smaller (less than 1%) than the influence of the substrate structures (acrolein vs. cyclohexenone) and the choice of the reference starting materials (i.e., **CPop** vs. simple Me_2Cu^- as in ref. [16]). For examples of the structural, method, and basis-set effects on KIEs for simple models, see Figure 7. (We thank M. Yamanaka for some calculations.)

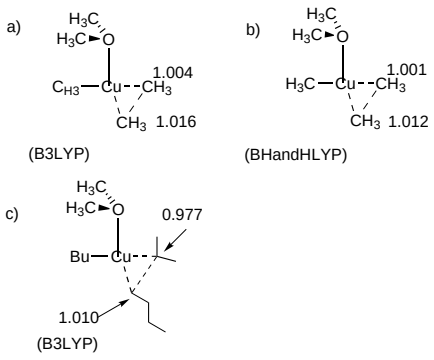

Figure 7. ^{13}C isotope effects at $-78\,^{\circ}$C, scale factor 0.963, 631A basis set, with tunneling corrections. Reference starting materials are Me_2Cu in a and b, and Bu_2Cu^- in c.

[50] See P. Czyryca, P. Paneth, *J. Org. Chem.* **1997**, *62*, 7305–7309.

[51] E. Nakamura, M. Nakamura, Y. Miyachi, N. Koga, K. Morokuma, *J. Am. Chem. Soc.* **1993**, *115*, 99–106.

[52] For pertinent references on cyanocuprates, see: a) S. H. Bertz, K. Nilsson, K. Ö. Davidson, J. P. Snyder, *Angew. Chem.* **1998**, *110*, 327–331; *Angew. Chem. Int. Ed.* **1998**, *37*, 314–317; b) T. L. Stemmler, T. M. Barnhart, J. E. Penner-Hahn, C. E. Tucker, P. Knochel, M. Böhme, G. Frenking, *J. Am. Chem. Soc.* **1995**, *117*, 12489–12497.

[53] E. Nakamura, I. Kuwajima, *J. Am. Chem. Soc.* **1984**, *106*, 3368–3370; Y. Horiguchi, S. Matsuzawa, E. Nakamura, I. Kuwajima, *Tetrahedron Lett.* **1986**, *27*, 4025–4028; E. Nakamura, S. Matsuzawa, Y. Horiguchi, I. Kuwajima, *Tetrahedron Lett.* **1986**, *27*, 4029–4032; S. Matsuzawa, Y. Horiguchi, E. Nakamura, I. Kuwajima, *Tetrahedron Lett.* **1989**, *45*, 349–362.

[54] See also: E. J. Corey, N. W. Boaz, *Tetrahedron Lett*, **1985**, *26*, 6015–6018; E. J. Corey, N. W. Boaz, *Tetrahedron Lett*, **1985**, *26*, 6019–6022; A. Alexakis, J. Berlan, Y. Besace, *Tetrahedron Lett*. **1986**, *27*, 1047–1050; review: E. Nakamura, *Organocopper Reagents* (Ed.: R. J. K. Taylor), Oxford University Press, **1994**, Chapter 6, pp. 129–142.

[55] B. L. Feringa, M. Pineschi, L. A. Arnold, R. Imbos, A. H. M. de Vries, *Angew. Chem.* **1997**, *109*, 2733–2736; *Angew. Chem. Int. Ed. Engl.* **1997**, *36*, 2620–2623; A. K. H. Knoobel, I. H. Escher, A. Pfaltz, *Synlett* **1997**, 1429–1431; Y. Nakagawa, M. Kanai, Y. Nagaoka, K. Tomioka, *Tetrahedron* **1998**, *54*, 10295–10307.

[56] B. E. Rossiter, N. M. Swingle, *Chem. Rev.* **1992**, *92*, 771–806.

Received: September 22, 1998 [F1359]